DARU Journal of Pharmaceutical Sciences (2019) 27:673–681
https://doi.org/10.1007/s40199-019-00301-3

RESEARCH ARTICLE

Improved transdermal delivery of cetirizine hydrochloride using polymeric microneedles

Muhammad Sohail Arshad[1] · Sana Hassan[1] · Amjad Hussain[2] · Nasir Abbas[2] · Israfil Kucuk[3] · Kazem Nazari[4] · Radeyah Ali[4] · Suleman Ramzan[4] · Ali Alqahtani[4] · Eleftherios G. Andriotis[5] · Dimitris G. Fatouros[5] · Ming-Wei Chang[6,7,8] · Zeeshan Ahmad[4]

Received: 15 May 2019 / Accepted: 13 September 2019 / Published online: 19 October 2019

Abstract

Purpose The aim of this study was to design and characterize microneedle patch formulation containing cetirizine hydrochloride.
Methods Chitosan was co-formulated with cetirizine hydrochloride. Transdermal patches were prepared by casting this solution to microneedle molds. Control patches were formulated by casting this solution to a plain cuvet of same area as mold but lacking microneedles. An array of methods namely; differential scanning calorimetry (DSC), thermogravimetric analysis (TGA) and scanning electron microscopy (SEM) were employed for the characterization of the films and the microneedles accordingly whereas *in vitro* permeation studies were conducted across rat skin. Light microscopy was performed to assess any histological changes upon microneedles application onto the rat skin.
Results The patches had a reproducible thickness (0.86 ± 0.06 mm) and folding endurance. Both the blank and drug loaded patches had 100 microneedles each of 300 micrometre length. In addition, the microneedle patches were ascribed with a two-fold increase in drug permeation across rat skin in the presence of microneedles as compared to the control formulations. Histological examination confirms a minimal invasion of the skin conferred by the microneedles.
Conclusion The microneedle patches serve as an alternate route of drug administration in patients with nausea and swelling difficulties.

Keywords Microneedles · Transdermal Drug delivery · Cetirizine Hydrochloride

Introduction

Transdermal drug delivery (TDD) refers to the administration of drug across the skin in order to impact the adjacent tissues or to approach the blood stream [1]. Transdermal drug delivery is advantageous as it offers; ease of application, affluent removal of dosage form, improved patient compliance (pain free) and the ability to control the rate of drug release. The 'hepatic first pass effect' is also avoided and drug absorption is not affected by factors such as pH, drug-food interaction, and enzyme activity with this route of administration [2, 3]. Nevertheless, some disadvantages are linked to TDD system

✉ Zeeshan Ahmad
zeeshan.ahmad@dmu.ac.uk

[1] Faculty of Pharmacy, Bahauddin Zakariya University, Multan, Pakistan

[2] College of Pharmacy, University of the Punjab Lahore, Lahore, Pakistan

[3] Faculty of Engineering and natural sciences, Bursa Technical University, Bursa, Turkey

[4] The Leicester School of Pharmacy, De Montfort University, Leicester, UK

[5] Department of Pharmacy, Aristotle University of Thessaloniki, Thessaloniki, Greece

[6] Department of Biomedical Engineering, Key Laboratory of Ministry of Education, Zhejiang University, Hangzhou 310027, People's Republic of China

[7] Zhejiang Provincial Key Laboratory of Cardio-Cerebral Vascular Detection Technology and Medicinal Effectiveness Appraisal, Zhejiang University, Hangzhou 310027, People's Republic of China

[8] Nanotechnology and Integrated Bioengineering Centre, University of Ulster, Jordanstown Campus, Newtownabbey, Northern Ireland BT37 0QB, UK

(TDDS); the barrier function of skin restricts the entry of polar hydrophilic drug substances, only potent lipophilic drugs are a suitable candidate for this route of administration. Drug permeation is affected by various factors including the age of skin, site of application and any pre-existing skin conditions [4].

In recent years, substantial progress has been made in the field of transdermal drug delivery [4–6] which enables prompt the systemic delivery of hydrophilic polar drug substance. One such example includes microneedle based TDDS, designed to modify the barrier function by disrupting the layer of skin in order to allow hydrophilic molecules to pass into the blood stream. [7]. The length of needles should be of such size that they penetrate through the dermis but prevent the stimulation of dermal nerves [8].

Microneedles utilized for drug delivery are fabricated from metal, ceramics, polymers or silicon [9, 10]. A variety of techniques are used to fabricate microneedles. These include; a) micromolding of template forming materials such as silicon, polydimethylsiloxane, or ceramics [11] b) lithography at glass transition of a material [12], c) twisted light with spin (metallic microneedles) [13] d) droplet born air blowing method [14].

Transdermal drug delivery through Microneedles approach is achieved by one of the following routines; a) applying blank microneedle to the skin followed by the placement of a patch, b) medicated polymeric patch with microneedle [15], or c) a metallic microneedles coated with drug solutions [16]. This approach is suitable for the systemic delivery of drug molecules having high weight and higher water solubility.

Cetirizine hydrochloride, an anti-histaminic drug used for the treatment of hay fever, angioedema's and urticarial problems and allergies [17] was used as model drug in this study. With a partition coefficient value of 1.5, the drug is likely to have a limited penetration through intact. Since, therapeutic conditions often demand long time administration of cetirizine this may result in non-compliance amongst the patients. Microneedle based transdermal delivery approach may provide an elevated level of drug without affecting the daily routine.

The aim of this study was to design polymeric microneedle patches containing cetirizine and evaluate the effect of microneedles on drug permeation. The patch formulation with or without microneedles were prepared using chitosan and sodium alginate and drug penetration studies were performed using rat skin.

Materials

Cetirizine Hydrochloride was received as a gift from Tagma Pharma Lahore Pakistan. Chitosan and sodium alginate were purchased from Sigma Aldrich, Germany. Acetic acid, Sodium hydrochloride, Hydrochloric Acid, were purchased from Merck, Germany. Distilled water was obtained from an in-house facility.

Fabrication of template mold

The fabrication of the silicone rubber template includes the following steps: i) Preparation of the stainless steel microneedle master mould by conventional machining methods, including grinding, electro-discharge machining, and electro-polishing ii) Preparation of silicone rubber Dow Corning Sylgard 184 silicone:hardener 10:1 iii) Casting of the mixed silicone liquid over the stainless steel microneedle master mould iv) Heating the silicone liquid to 80 ^{o}Cfor 1 h and v) de-mould the cured microneedle template from the master mould [18].

Methods

Chitosan was dissolved in an acetic acid aqueous solution (1% v/v) to produce polymeric solution 2% (w/v). This solution was then dialyzed through a dialyzing tube (cut off size 14 k Dalton) at temperature 37 ± 0.5°C against deionized water until its pH increased to 6. This solution was dried (at 37°C) by placing in a water bath until the solution of chitosan was 10 percent by weight (i.e. 10% w/v) [19].

Neutralized chitosan solution (10% w/v) was casted onto the pre-fabricated microneedle molds of polydimethylsiloxane containing 10 × 10 cavities each of 300 micrometer depth. The molds were centrifuged at 3500 rpm for 1 minute to force the chitosan solution into the cavities of the mold. Casting and centrifugation cycle was repeated twice to ensure that mold is properly filled with chitosan solution. The excess solution was removed from the surface of mold and filled solution was dried at room temperature (25 ± 2°C) for 24 hour [20].

For sodium alginate microneedles the polymer solution of 20% w/w with or without drug was casted centrifuged and dried as described for chitosan microneedles [21, 22]. Transdermal patches of same dimensions were also prepared by casting the equivalent volume of formulation solution(s) in the mold without centrifugation.

The drug loading to the polymer matrix was achieved by dissolving the specified amount of cetirizine HCl to the respective polymer solutions (Table 1). The drug concentrations were maintained at such levels that phase separation was not reached.

Characterization studies of microneedles

Evaluation of films: folding, and thickness

Prepared transdermal patches and microneedle patches were tested for uniformity in thickness using Vernier's caliper. Moreover, the dosage forms were tested for integrity after folding.

Table 1 Composition of different formulations

Formulation	Blank MN	Drug loaded MN	Drug loaded Patch	Blank MN	Drug loaded MN	Drug loaded Patch
Sodium Alginate (% w/v)	20	20	20	-	-	-
Chitosan (% w/v)	-	-	-	10	10	10
Polymer to Drug ratio	-	1:5	1:5	-	1:4	1:4

Scanning electron microscopy test of microneedle formulations

The morphology of microneedle patches were examined for needle size, shape and other physical attributes using scanning electron microscope (SEM) (Oxford Instruments, UK). The specimens were sputter coated with gold solution to obtain a clear image of the object.

Differential scanning calorimetry

This technique was used to record enthalpic change in the constituent polymer(s), cetirizine hydrochloride and the prepared microneedle following increase in its temperature. Each of these materials were heated to 300°C at 10°C. min^{-1} using a DSC equipment previously calibrated at same rate up to 450°C for temperature and heat flow using Nickel and Zinc at standard materials [21, 23] .

Thermogravimetry analysis

Thermogravimetric analysis (TGA) records weight loss in the samples following increase in temperature. The samples including chitosan, sodium alginate, cetirizine Hydrochloride and prepared microneedles were heated from 25°C to 350°C at a heating rate of 10°C.min^{-1} and weight loss was recorded to evaluate physical stability of the materials [24, 25].

FTIR

Fourier transform infra-red (FTIR) spectroscopic analysis records the vibration of different functional groups in the samples following interactions with light radiation over a specific wavelength range (400-4000 cm^{-1}) [26, 27].

In vitro delivery of cetirizine drug across rat skin from sodium alginate microneedles and patch of sodium alginate

The study was performed after an approval of protocol from departmental Animal Ethical Committee BZU (49/PEC dated 2-1-2018). Rats weighting 150 ± 25 g were used as experimental animals for this study. The animals were kept at ambient temperature and provided with a free access to food and water. The animals were euthanized by injecting higher doses of anesthetic ketamine (100 mg/kg IP) followed by decapitation.

Drug permeation through the rat skin was investigated by using modified Franz cell, comprising of donor and acceptor compartments having a permeation area of 1 cm^2. Briefly, the acceptor compartment was filled with freshly prepared Phosphate buffer solution (pH 7.4) and its temperature was maintained at 37°C by circulating water in the jacket of acceptor chamber in order to simulate the physiologic conditions. An excised rat skin (1 cm^2), previously defatted by dipping in hot water followed by teasing the dermis from epidermis, and hydrated in phosphate buffer (pH 5.6) in order to establish equilibrium with the dilution medium was clamped carefully between the donor and recipient chambers. Transdermal patch formulations (plain and microneedle patches) were applied to rat skin and the solution in recipient compartment was stirred at 600 rpm in order to ensure a prompt mass transfer following permeation. Aliquots of 1 mL were removed from the recipient compartment at predetermined time intervals over a time period of 8 h and same volume of buffer solution (blank) was replaced in order to maintain the sink conditions. Drug contents of each sample were then measured by spectrophotometric method [28, 29]. Briefly, a stock solution of cetirizine hydrochloride 1% w/v was prepared using buffer solution by dissolving 1.0 ± 0.002 g in volumetric flask 100 ± 0.01 ml. this solution was sonicated

Table 2 Evaluation of microneedle thickness and folding

Evaluation test	Chitosan microneedle	Sodium alginate microneedle
Folding endurance	120	74
Thickness of microneedle patch	9.1 ± 4.33 mm	9.1 ± 6.77 mm
Width of the microneedle patch	0.86 ± 0.06 mm	0.81 ± 0.07 mm
Appearance of microneedle film	Smooth surface appearance	Rough surface appearance
Polymer solution color	Transparent light yellowish	Transparent light brownish

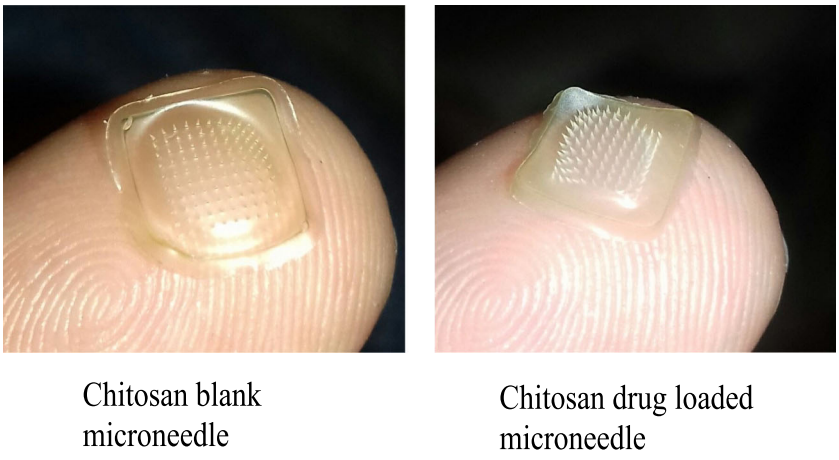

Fig. 1 Photographic images of microneedle patches prepared from chitosan.

for 5 min to ensure complete dissolution of drug. A working standard (100 μg.ml^{-1}) was then prepared by diluting the stock solution (1:100). Different Dilutions with drug concentration 5-100 μg.ml^{-1} were prepared and absorption was recorded at 244 nm using UV visible spectrophotometer (Perkin elmer, USA). Light Absorption was plotted as a function of concentration and fitted with linear regression equation. This equation was then used to determine the drug concentration from unknown samples [30, 31]. Diffusion of cetirizine from polymeric microneedles and patch was recorded through rat skin using modified Franz cell [19, 29].

Histological studies

After piercing with microneedle patches, the excised skin tissues were fixed in ethanol 70% w/v for 72 h and sliced with microtome [32]. The sliced tissues were examined under a light microscope for the integrity of the rat epidermis.

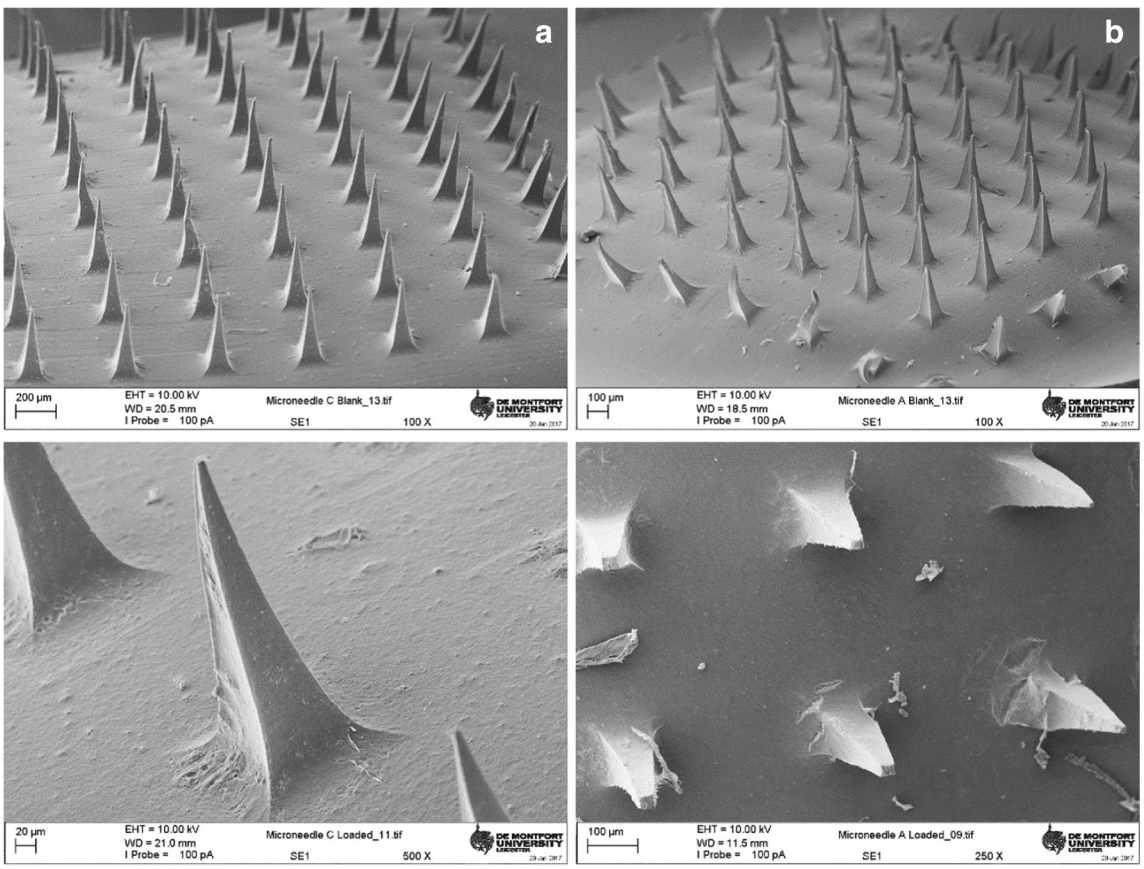

Fig. 2 Scanning electron micrographs of (left) chitosan and (Right) sodium alginate-based microneedle films; (Top) blank polymer microneedles (bottom) cetirizine loaded polymeric microneedle patch films

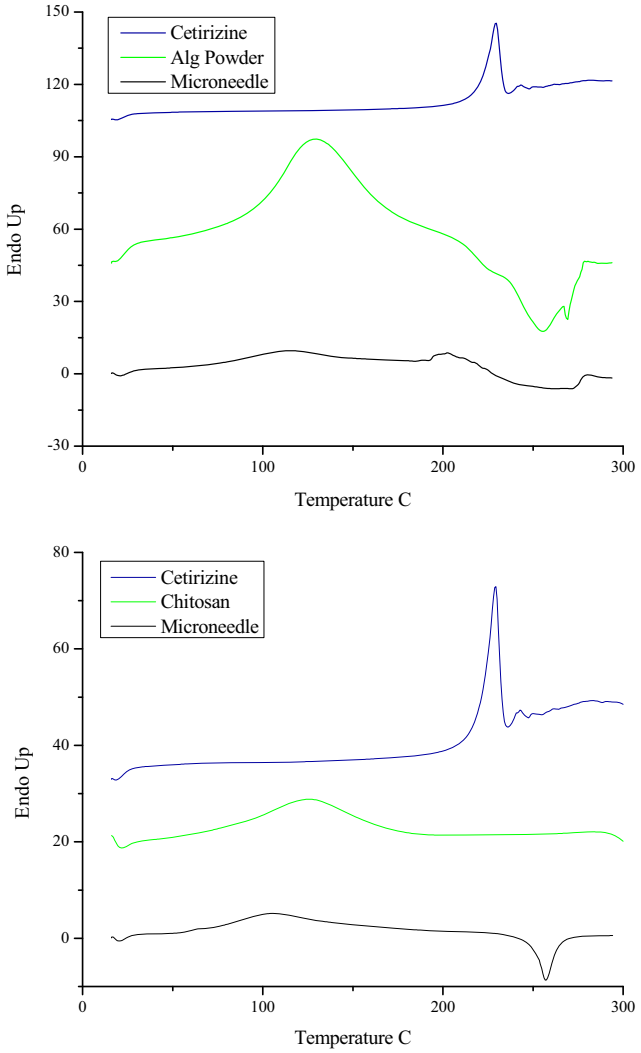

Fig. 3 DSC thermograms of (Top) cetirizine HCl, sodium alginate powder and microneedle patches containing sodium alginate and cetirizine HCl, (Bottom) cetirizine HCl, Chitosan powder and microneedle patches containing chitosan and cetirizine HCl

Results and discussion

Evaluation of films: folding, and thickness

Chitosan and sodium alginate microneedles thickness was observed 9.1 ± 4.3 mm. The folding endurance of microneedle patches were observed through the flat side as well as needles side of the film. Folding endurance for chitosan the flat side exceed 120 while the sodium alginate counterpart it was 75 folding before being damaged (Table 2). Chitosan microneedles were more flexible as compared to the sodium alginate microneedles. The results suggest an acceptable operational performance of the patches.

The needle side folding of film caused significant damage to the needles following 10-15 folding damaged in both sodium alginate microneedles and chitosan microneedles. The results point to significant care to prevent needle side folding [33].

Optical microscopic images of the microneedle films depict the needle projections being smaller than fingerprints in the background (Fig. 1). Inclusion of cetirizine in the patches did not affect the shape of the microneedles.

Scanning electron microscopy test of microneedle formulations

Scanning electron microscopic studies were performed to get an insight on the microneedle patches morphology. The microneedle patch appeared as a smooth film with evenly distributed microneedle projections (N = 100). Each of the needles had a four cornered base with a facet width of 100 micrometers which narrows to a fine tip over a length of 300 microns (Fig. 2). A closer look at the patches with broken microneedles revealed a hollow tube-like structure of the chitosan needles while the alginate counterparts were filled [29, 34]. It is noteworthy to state that the results from optical microscopy of freshly prepared drug loaded microneedles patches of both polymers depict an acceptable morphology. However, following transportation to other facility for SEM, these patches undergo mechanical stress which result in occasional damage to the microstructures.

Differential scanning calorimetry

DSC thermograms of cetirizine demonstrate a sharp endothermic peak at 220°C with heat of fusion ΔH 161.29 $J.g^{-1}$. These results confirm the crystalline nature of the drug. The thermograms of sodium alginate showed endothermic peak at 100°C which manifest the dehydration from the polymer while an exothermic peak at 240-60°C was observed due to pyrolysis reaction [35, 36] (Fig. 3 top). A broadened endothermic peak with relatively lower intensity recorded at ~195°C indicates the melting of cetirizine HCl. A tailing effect in this endothermic peak suggests that melting of cetirizine HCl is coupled with another thermal event possibly the decomposition of accompanying polymer.

The thermogram of chitosan showed a broad endothermic peak with onset temperature ~80°C relating to release of water while an exothermic peak at ~300°C manifests decomposition of amine (GlcN) units of the polymer (Fig. 3 bottom) [37]. These thermal events i.e. dehydration and decomposition were recorded at lower onset temperatures 70 and 250°C respectively, in microneedle patches prepared from chitosan and cetirizine. This reflects a plasticizing effect of the cetirizine HCl. Moreover, the thermogram of drug loaded chitosan based microneedle patches films did not show melting peak of the cetirizine HCl suggesting a non-crystalline form of the drug.

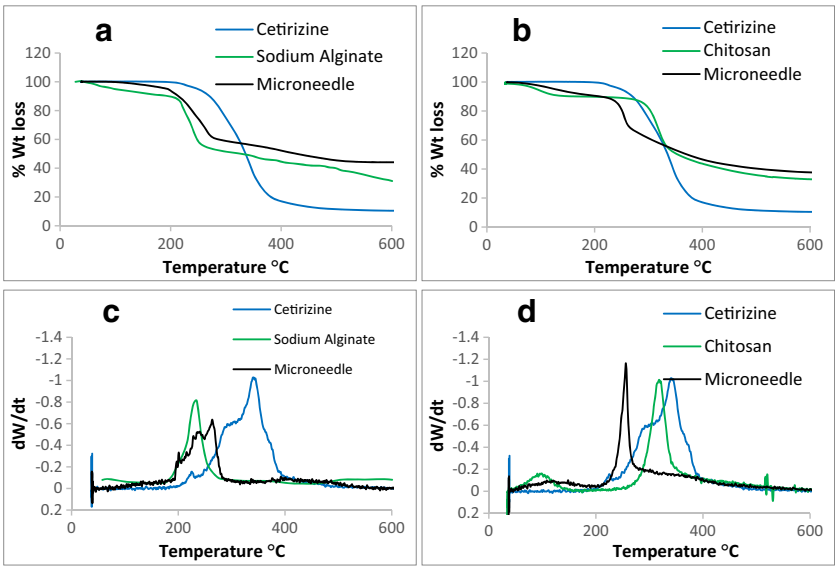

Fig. 4 TGA of A) Sodium Alginate, cetirizine and cetirizine loaded sodium alginate-based microneedle patch and B) Chitosan, cetirizine and cetirizine loaded chitosan based microneedle patch. Part C & D show first derivative of sodium alginate and chitosan thermograms, respectively.

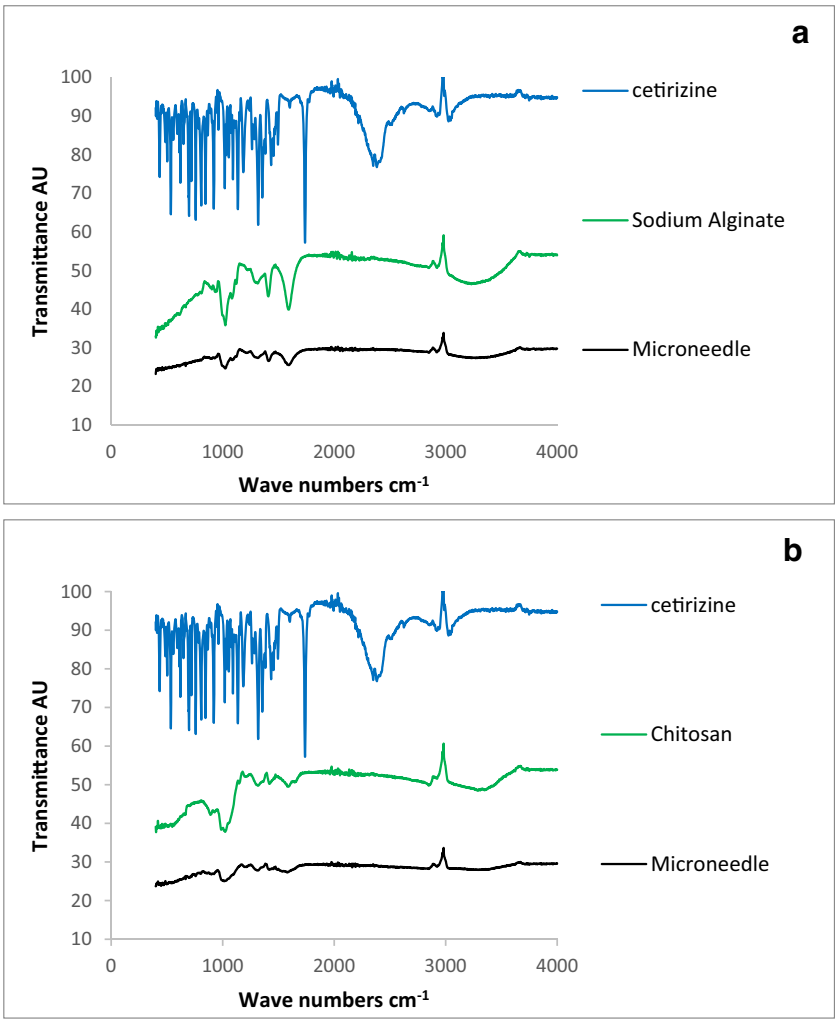

Fig. 5 FTIR spectra of A) Sodium Alginate, cetirizine and cetirizine loaded sodium alginate based microneedle patch and B) Chitosan, cetirizine and cetirizine loaded chitosan based microneedle patch.

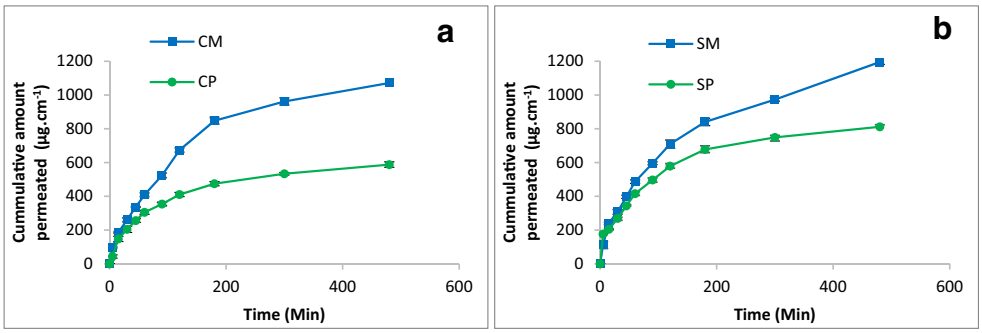

Fig. 6 Cumulative amount of drug permeated through rat skin A) Chitosan films B) Sodium Alginate films

Thermo-gravimetric analysis

The gravimetric analysis of cetirizine revealed no weight loss in cetirizine up to 200°C which reflects thermal stability of the drug. At temperatures above 220°C there is a step like decrease in mass suggesting its degradation (Fig. 4).

TG thermograms of sodium alginate showed weight loss of 13, 33 and 20% over the temperature ranges of 100-200, 200-266 and 266-600°C, respectively. Similarly, the weight changes in sodium alginate films containing cetirizine with the temperature were triphasic; around 7% weight loss recorded over a temperature range of 120-200°C, approximately 30% over 200-280°C and another 15% weight loss over a temperature range 300-550°C (Fig. 4A). The first stage of weight loss is linked to the removal of water from the samples while the second phase account for combustion of carbon in the polymer followed by further decay of material at high temperature.

Weight changes recorded from TGA of chitosan read; approximately 10% loss over 50-127°C (Phase I), 35% loss between 220-330°C (Phase II), followed by 20% weight loss upto 600°C (Phase III). The results from thermogravimetric analysis of cetirizine HCl loaded patches mimic those found with the polymer except with a slower gradient of phase I and early onset of Phase II.

First derivative of % weight loss described changes in the gradients of sample weight with the temperature. The composite films of sodium alginate showed lower gravimetric gradient than the individual components where it was noted otherwise for chitosan counterpart (Fig. 4C &D).

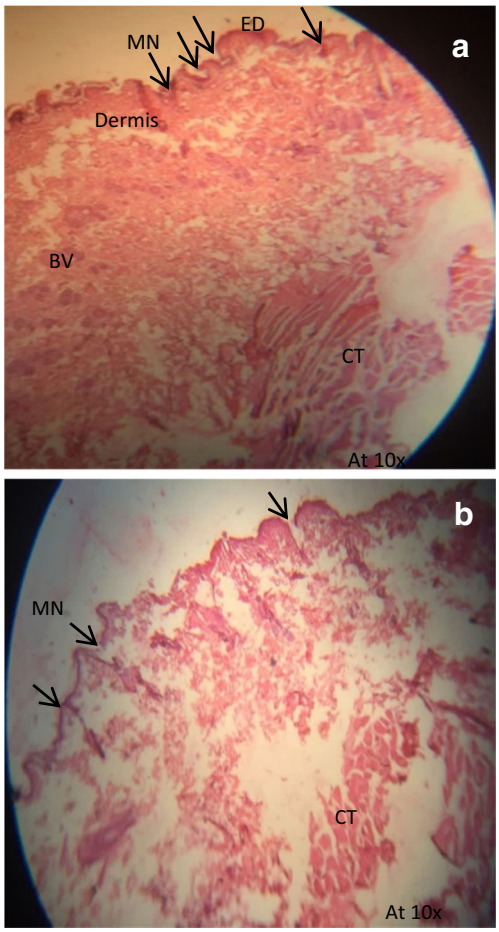

Fig. 7 Microscopic images of the excised skin pierced with sodium alginate microneedle patch.

FTIR

The FTIR spectrum of cetirizine showed the peak at 1457 cm^{-1} due to vibrations of C-Cl, a sharp peak at 1740 cm^{-1} is attributed to the stretching of the C=O group of the COOH, stretching vibration NH manifest a spectral peak at 2384, a broad peak at 3200-3600 cm^{-1} arises from dimer O-H stretching vibrations of COOH.

The Sodium Alginate spectrum showed peaks at 1596, 1409 and 1024 cm^{-1} due to stretching vibration of aromatic C-C bonds, carboxylate group and carbonyl group respectively (Fig. 5A). The FTIR spectrum of chitosan manifest peaks at 1023,1320, 1581, 3349 cm^{-1} due to the vibration of carbonyl, hydroxyl (O-H), N-H of amine, and OH functional groups, respectively (Fig. 5B). Following film formulation, the position of these peaks was slightly shifted to higher wavelengths suggesting a loose packing of these groups which require low energy for these vibrations. One may question that the spectra of composite films were influenced by the polymer counterpart, a justification to this observation is that the polymer components are ≤80% of the formulation. No additional peak

was recorded in the FTIR spectrum of transdermal patches implying that there wasn't a chemical reaction between the polymer and drug.

Ex vivo delivery of cetirizine

The time profile of cetirizine permeation across rat skin is measured by Franz diffusion cell using spectrophotometric method. Spectrophotometric absorption data follows a linear regression function ($y = mx + b$) over a concentration range 10-60 $\mu g.ml^{-1}$. Correlation coefficient R^2 value 0.998 confirms that the model equation could be used to describe the data.

For chitosan patch formulation a steady state was observed at 200 min while the microneedle counterpart depicts a plateau at significantly higher concentration i.e. 450 min (Fig. 6A). The steady state concentration from sodium alginate patch and microneedle patch was 749 and 973 $\mu g/cm^2.hr$, respectively (Fig. 6B). It is reasonable to describe that microneedle based patch of chitosan and sodium alginate has ~45 and 25% higher drug concentration as compared to control (plain polymer patch formulation), after 6 h of application.

Histological examination of the excised skin

Histological examination of the skin samples previously administered with microneedle patch revealed the presence of epidermis (ED) with discontinuation, intact dermis deeper inside blood vessels (BV) and skeletal muscles connective tissue (CT) Fig. 7A. Furthermore, the presence of additional channels in the proximity of the outer surface of excised skin evidence a breakdown in the physiologic barrier by the microneedles. Other features of the skin tissue such as intact connective tissue signifies that microneedle induced only a controlled perturbation in the top layer of skin Fig. 7B. Histological examination confirms a minimal invasion of the skin conferred by the microneedles which provides channels for the transfer of drug substance across the skin.

Conclusion

Microneedles composed of chitosan and sodium alginate with drug to polymer ratios 1:4 and 1:5, respectively prepared using molding and casting technique were evaluated for integrity and permeation enhancement of entrapped drug. Both the chitosan as well as sodium alginate-based patches had sufficient plasticity and folding endurance implying their application for the transdermal drug delivery. Furthermore, the results of DSC and FTIR studies revealed that none of these materials show chemical incompatibility with drug. Therefore, these natural biodegradable polymeric materials are suitable for formulation development. Since molded polymeric films retain the needle morphology on drying, one can presume their penetration through stratum corneum provide a facilitated path for the drug substances.

The results of permeation studies confirm that polymeric microneedle films significantly improve the transdermal permeation of cetirizine as compared the control i.e. polymeric films without microneedles. Efficient permeation profile refers to successful formulation development with promising therapeutic outcomes.

Acknowledgements The authors acknowledge the financial support provided by Higher Education Commision of Pakistan under National Research Program for Universities (NRPU) vide No: 7401/Punjab/NRPU/R&D/HEC/2017.

Authors' contributions All authors contributed to the preparation of the manuscript and the study (i.e. through various streams be it planning, experiments, analysis of data, data preparation etc).

Compliance with ethical standards

Conflict of Interest The authors have no conflict of interests.

References

1. Ranade VV, Hollinger MA. Drug delivery systems. FL, USA: CRC press Boca Raton; 2004.
2. Naik A, Kalia YN, Guy RH. Transdermal drug delivery: overcoming the skin's barrier function. Pharm Sci Technol To. 2000;3(9):318–26.
3. Prausnitz MR, Langer R. Transdermal drug delivery. Nat Biotechnol. 2008;26(11):1261–8.
4. Patel D, Chaudhary SA, Parmar B, Bhura N. Transdermal drug delivery system: a review. The Pharma Innovation. 2012;1(4).
5. Rasekh M, Karavasili C, Soong YL, Bouropoulos N, Morris M, Armitage D, et al. Electrospun PVP–indomethacin constituents for transdermal dressings and drug delivery devices. Int J Pharm. 2014;473(1):95–104. https://doi.org/10.1016/j.ijpharm.2014.06.059.
6. Ahmad Z, Stride E, Edirisinghe M. Novel preparation of transdermal drug-delivery patches and functional wound healing materials. J Drug Target. 2009;17(9):724–9. https://doi.org/10.3109/10611860903085386.
7. Larrañeta E, Lutton RE, Woolfson AD, Donnelly RF. Microneedle arrays as transdermal and intradermal drug delivery systems: Materials science, manufacture and commercial development. Mat Sci Eng: R: Reports. 2016;104:1–32.
8. Ita K. Dissolving microneedles for transdermal drug delivery: Advances and challenges. Biomed Pharmacother. 2017;93:1116–27. https://doi.org/10.1016/j.biopha.2017.07.019.
9. Larrañeta E, McCrudden MT, Courtenay AJ, Donnelly RF. Microneedles: a new frontier in nanomedicine delivery. Pharm Res. 2016;33(5):1055–73.
10. Khan H, Mehta P, Msallam H, Armitage D, Ahmad Z. Smart microneedle coatings for controlled delivery and biomedical analysis. J Drug Target. 2014;22(9):790–5. https://doi.org/10.3109/1061186X.2014.921926.
11. Bystrova S, Luttge R. Micromolding for ceramic microneedle arrays. Microelectron Eng. 2011;88(8):1681–4.

12. Lee K, Jung H. Drawing lithography for microneedles: a review of fundamentals and biomedical applications. Biomaterials. 2012;33(30):7309–26.
13. Omatsu T, Chujo K, Miyamoto K, Okida M, Nakamura K, Aoki N, et al. Metal microneedle fabrication using twisted light with spin. Opt Express. 2010;18(17):17967–73. https://doi.org/10.1364/OE.18.017967.
14. Kim JD, Kim M, Yang H, Lee K, Jung H. Droplet-born air blowing: novel dissolving microneedle fabrication. J Control Release. 2013;170(3):430–6. https://doi.org/10.1016/j.jconrel.2013.05.026.
15. Park J-H, Allen MG, Prausnitz MR. Polymer microneedles for controlled-release drug delivery. Pharm Res. 2006;23(5):1008–19.
16. Haj-Ahmad R, Khan H, Arshad M, Rasekh M, Hussain A, Walsh S, et al. Microneedle Coating Techniques for Transdermal Drug Delivery. Pharmaceutics. 2015;7(4):486.
17. Goindi S, Kumar G, Kumar N, Kaur A. Development of novel elastic vesicle-based topical formulation of cetirizine dihydrochloride for treatment of atopic dermatitis. AAPS PharmSciTech. 2013;14(4):1284–93.
18. Wang M, Hu L, Xu C. Recent advances in the design of polymeric microneedles for transdermal drug delivery and biosensing. Lab Chip. 2017;17(8):1373–87.
19. Chen M-C, Ling M-H, Lai K-Y, Pramudityo E. Chitosan microneedle patches for sustained transdermal delivery of macromolecules. Biomacromolecules. 2012;13(12):4022–31.
20. Chang C, Wang Z-C, Quan C-Y, Cheng H, Cheng S-X, Zhang X-Z, et al. Fabrication of a novel pH-sensitive glutaraldehyde cross-linked pectin nanogel for drug delivery. J Biomater Sci Polym Ed. 2007;18(12):1591–9. https://doi.org/10.1163/156856207794761925.
21. Demir YK, Akan Z, Kerimoglu O. Characterization of Polymeric Microneedle Arrays for Transdermal Drug Delivery. PLoS ONE. 2013;8(10):e77289. https://doi.org/10.1371/journal.pone.0077289.
22. Seok H-y, Suh H, Baek S, Kim Y-C. Microneedle applications for DNA vaccine delivery to the skin. DNA Vaccines: Methods and Protocols. 2014:141-58.
23. Ma Y, Gill HS. Coating Solid Dispersions on Microneedles via a Molten Dip-Coating Method: Development and In Vitro Evaluation for Transdermal Delivery of a Water-Insoluble Drug. J Pharm Sci. 2014;103(11):3621–30.
24. Moga KA, Bickford LR, Geil RD, Dunn SS, Pandya AA, Wang Y, et al. Rapidly–dissolvable microneedle patches via a highly scalable and reproducible soft lithography approach. Adv Mater. 2013;25(36):5060–6.
25. Martin C, Allender CJ, Brain KR, Morrissey A, Birchall JC. Low temperature fabrication of biodegradable sugar glass microneedles for transdermal drug delivery applications. J Control Release. 2012;158(1):93–101.
26. Migalska K, Morrow DI, Garland MJ, Thakur R, Woolfson AD, Donnelly RF. Laser-engineered dissolving microneedle arrays for transdermal macromolecular drug delivery. Pharm Res. 2011;28(8):1919–30.
27. Gittard SD, Ovsianikov A, Akar H, Chichkov B, Monteiro-Riviere NA, Stafslien S et al. Two Photon Polymerization-Micromolding of Polyethylene Glycol-Gentamicin Sulfate Microneedles. Adv Eng Mate. 2010;12(4).
28. Auner BG, Valenta C, Hadgraft J. Influence of phloretin and 6-ketocholestanol on the skin permeation of sodium-fluorescein. J Control Release. 2003;89(2):321–8.
29. Xie Y, Xu B, Gao Y. Controlled transdermal delivery of model drug compounds by MEMS microneedle array. Nanomedicine. 2005;1(2):184–90.
30. Wankhede S, Lad K, Chitlange S. Development and validation of UV-spectrophotometric methods for simultaneous estimation of cetirizine hydrochloride and phenylephrine hydrochloride in tablets. Int J Pharm Sci Drug Res. 2012;4(3):222–6.
31. Bhatia NM, Ganbavale SK, More HN. Spectrophotometric estimation of ambroxol hydrochloride and cetirizine hydrochloride in tablets. Asian J Pharm. 2014;2(3).
32. van Essen HF, Verdaasdonk MA, Elshof SM, de Weger RA, van Diest PJ. Alcohol based tissue fixation as an alternative for formaldehyde: influence on immunohistochemistry. J Clin Pathol. 2010;63(12):1090–4. https://doi.org/10.1136/jcp.2010.079905.
33. Davis SP. Hollow microneedles for molecular transport across skin: Georgia Institute of Technology; 2004.
34. Park J-H, Allen MG, Prausnitz MR. Biodegradable polymer microneedles: fabrication. mechanics and transdermal drug delivery. J Control Release. 2005;104(1):51–66.
35. Jana S, Trivedi M, Tallapragada RM, Branton A, Trivedi D, Nayak G, et al. Characterization of Physicochemical and Thermal Properties of Chitosan and Sodium Alginate after Biofield Treatment. Pharm Anal Acta. 2015;10(6).
36. Soares JP, Santos J, Chierice GO, Cavalheiro E. Thermal behavior of alginic acid and its sodium salt. Eclética Química. 2004;29(2):57–64.
37. Guinesi LS, Cavalheiro ETG. The use of DSC curves to determine the acetylation degree of chitin/chitosan samples. Thermochim Acta. 2006;444(2):128–33.